



Article

# Whole Transcriptome Analysis of Substantia Nigra in Mice with MPTP-Induced Parkinsonism Bearing Defective Glucocerebrosidase Activity

Tatiana Usenko <sup>1,2</sup> , Anastasia Bezrukova <sup>1,2</sup>, Margarita M. Rudenok <sup>3</sup>, Katerina Basharova <sup>1</sup>, Maria I. Shadrina <sup>3</sup>, Petr A. Slominsky <sup>3</sup>, Ekaterina Zakharova <sup>4,\*</sup> and Sofya Pchelina <sup>1,2</sup>

- <sup>1</sup> Petersburg Nuclear Physics Institute Named by B.P. Konstantinov of National Research Centre «Kurchatov Institute», 188300 Gatchina, Russia; usenko\_ts@pnpi.nrcki.ru (T.U.); bezrukova\_ai@pnpi.nrcki.ru (A.B.); basharova\_ks@pnpi.nrcki.ru (K.B.); pchelina\_sn@pnpi.nrcki.ru (S.P.)
- <sup>2</sup> Department of Molecular Genetic and Nanobiological Technologies, Pavlov First Saint-Petersburg State Medical University, 197022 Saint-Petersburg, Russia
- <sup>3</sup> Institute of Molecular Genetics, Russian Academy of Sciences, 123182 Moscow, Russia; rudenok@img.msk.ru (M.M.R.); shadrina@img.ras.ru (M.I.S.); slomin@img.ras.ru (P.A.S.)
- <sup>4</sup> Research Center for Medical Genetics, Laboratory of Hereditary Metabolic Diseases, 115522 Moscow, Russia
- \* Correspondence: zakharova@med-gen.ru

**Abstract:** Mutations in the *GBA1* gene represent the major genetic risk factor for Parkinson's disease (PD). The lysosomal enzyme beta-glucocerebrosidase (GCase) encoded by the *GBA1* gene participates in both the endolysosomal pathway and the immune response. Disruption of these mechanisms is involved in PD pathogenesis. However, molecular mechanisms of PD associated with *GBA1* mutations (GBA-PD) are unknown today in particular due to the partial penetrance of *GBA1* variants in PD. The modifiers of *GBA1* penetrance have not been elucidated. We characterized the transcriptomic profiles of cells from the substantia nigra (SN) of mice with co-injection with 1-methyl-4-phenyl-1,2,3,6-tetrahydropyridine (MPTP) and selective inhibitor of GCase activity (conduiritol- $\beta$ -epoxide, (CBE)) to mimic PD bearing GCase dysfunction (MPTP+CBE), mice treated with MPTP, mice treated with CBE and control mice treated with injection of sodium chloride (NaCl) (vehicle). Differential expression analysis, pathway enrichment analysis, and outlier detection were performed. Functional clustering of differentially represented transcripts revealed more processes associated with the functioning of neurogenesis, inflammation, apoptosis and autophagy in MPTP+CBE and MPTP mice than in vehicle mice, with a more pronounced alteration of autophagy processes in MPTP+CBE mice than in MPTP mice. The PI3K-Akt-mTOR signaling pathway may be considered a potential target for therapy in PD with GCase dysfunction.

**Keywords:** Parkinson's disease; transcriptome; 1-methyl-4-phenyl-1,2,3,6-tetrahydropyridine (MPTP); conduiritol- $\beta$ -epoxide (CBE); substantia nigra (SN)



**Citation:** Usenko, T.; Bezrukova, A.; Rudenok, M.M.; Basharova, K.; Shadrina, M.I.; Slominsky, P.A.; Zakharova, E.; Pchelina, S. Whole Transcriptome Analysis of Substantia Nigra in Mice with MPTP-Induced Parkinsonism Bearing Defective Glucocerebrosidase Activity. *Int. J. Mol. Sci.* **2023**, *24*, 12164. <https://doi.org/10.3390/ijms241512164>

Academic Editor: Hari Shanker Sharma

Received: 29 June 2023  
Revised: 21 July 2023  
Accepted: 26 July 2023  
Published: 29 July 2023



**Copyright:** © 2023 by the authors. Licensee MDPI, Basel, Switzerland. This article is an open access article distributed under the terms and conditions of the Creative Commons Attribution (CC BY) license (<https://creativecommons.org/licenses/by/4.0/>).

## 1. Introduction

Parkinson's disease (PD) is one of the most common neurodegenerative diseases, and is characterized by the degeneration of dopaminergic neurons (DN) of the midbrain accompanied by protein  $\alpha$ -synuclein accumulation [1,2]. Lysosomal enzyme beta-glucocerebrosidase (GCase), encoded by the *GBA1* gene, is significant for the pathogenesis of PD. Mono- and biallelic mutations in the *GBA1* gene have been recognized as the greatest genetic risk factor for PD [3–7]. Homozygous and compound heterozygous *GBA1* mutations result in the most common lysosomal storage disorder (LSD), Gaucher disease (GD), characterized by lysosphingolipid accumulation, presumably in blood macrophages. This is a complex clinical picture that, in the neuronopathic forms of the disease, also includes neurological symptoms [8]. GCase is the lysosomal enzyme involved in ceramide metabolism, and it

catalyzes the hydrolysis of glucosylceramide to glucose and ceramide. In its turn, ceramide is involved in neuronal function, immune response, autophagy, etc. [9–11].

Despite previous data demonstrating that PD associated with mutations in *GBA1* gene (GBA-PD) is associated with the impairment of processes encompassing the endolysosomal pathways, vesicular trafficking, lipid metabolism, and the cell stress response, not every carrier of *GBA1* mutations develops PD during their lifetime. Our previous study based on the comparative transcriptome analysis revealed a pronounced alteration of autophagy and immune response in GBA-PD compared to non-manifesting *GBA1* mutation carriers in peripheral blood monocyte-derived macrophages [12]. Additionally, we, and others, have previously demonstrated that mutations in the *GBA1* gene lead to a decrease in GCCase activity in the blood in *GBA1* mutation carriers independent of PD status [13–17]. Therefore, it is important to determine the additional modifiers that are responsible for the onset of PD in some *GBA1* mutation carriers.

Mice models based on the administration of MPTP (1-methyl-4-phenyl-1,2,3,6-tetrahydropyridine), which became the first neurotoxin used to mimic PD, are the most frequently used models recapitulating PD-like symptoms [18–21]. Condurotol- $\beta$ -epoxide (CBE) is used for inhibition of GCCase activity due to its forming covalent bonds with the catalytic site of the enzyme, causing accumulation of the GCCase substrates glucosylceramide and glucosylsphingosine. CBE has long been used to inhibit GCCase activity in an attempt to replicate GD-like features in rodents [22]. Recently, Mus and colleagues first demonstrated the possibility of using CBE with MPTP in creation of a PD mice model with partial deficiency of GCCase activity [23]. We have replicated the double toxic model (MPTP+CBE) using the presymptomatic PD mouse model described earlier [24] and combined a low dosage of MPTP (12 mg/kg, i.p. for 14 days) with a single CBE injection (100 mg/kg) [25].

Here, we first generated the transcriptomic profiles of substantia nigra (SN) cells for mice with coadministration of MPTP and CBE as described earlier [25], mice with administration of MPTP alone, CBE alone, and sodium chloride (NaCl) as a vehicle. We identified new patterns of change in gene expression profile, as well as processes that may be associated with the initiation of PD development in the presence of GCCase defects. We also conducted a comparative analysis of the transcriptomic dataset of differentially expressed genes (DEGs) obtained by us in the current study and earlier during the analysis of the transcriptome of the primary culture of macrophages derived from peripheral blood lymphocytes of patients with GBA-PD and controls [12].

Herein, abnormalities in the autophagy process, in particular in the PI3K-Akt-mTOR signaling pathway in MPTP+CBE mice, were demonstrated, suggesting that possible modifiers of the mammalian target of rapamycin (mTOR) may be suitable for targeted therapeutic interventions.

## 2. Results

### 2.1. Changes in the Transcriptome Attributed to the Dysfunction of GCCase

Pairwise comparison of data from the groups of mice with MPTP vs. NaCl (vehicle mice), mice with MPTP vs. CBE, mice with MPTP vs. MPTP+CBE, mice with MPTP+CBE vs. CBE, mice with MPTP+CBE vs. vehicle mice and mice with CBE vs. vehicle mice was made using the DESeq library in R. Analysis revealed the expression of genes whose levels differed by more than 1.5 times, with a  $p$ -value < 0.01 between compared groups. We identified 64 DEGs in SN from mice with MPTP vs. vehicle mice (40 upregulated DEGs, 24 downregulated DEGs), 23 DEGs in mice with MPTP vs. CBE (22 upregulated DEGs, 1 downregulated DEG), 6 upregulated DEGs and 2 downregulated DEGs in mice with MPTP+CBE vs. MPTP, 23 DEGs in mice with MPTP+CBE vs. CBE (16 upregulated DEGs, 7 downregulated DEGs), 37 DEGs in mice with MPTP+CBE vs. vehicle mice (21 upregulated DEGs, 16 downregulated DEGs) and 1 downregulated DEG in mice with CBE vs. vehicle mice (Figure 1, Tables S1–S6).

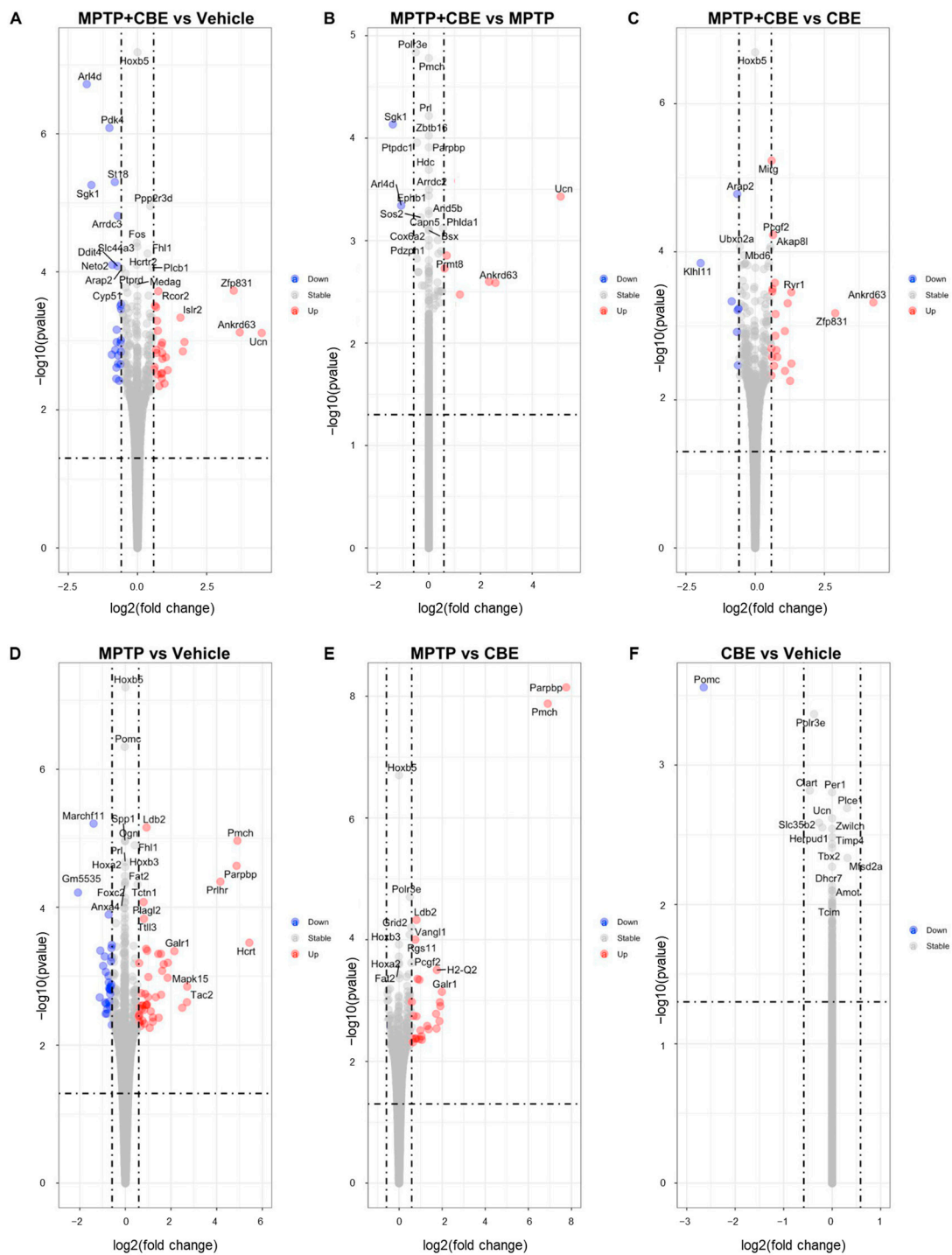


**Figure 1.** Volcano plot for DEGs between the studied groups (false discovery rate (FDR) < 0.05 and |fold change (FC)| > 1.5); the upregulated genes are represented by red dots and the downregulated genes are represented by blue dots. (A) MPTP+CBE vs. vehicle, (B) MPTP+CBE vs. MPTP, (C) MPTP+CBE vs. CBE, (D) MPTP vs. vehicle, (E) MPTP vs. CBE, (F) CBE vs. vehicle.

Following the results of the Venn Diagram, we found common alterations of gene expression between the groups (Table S7). Mice with MPTP vs. mice with CBE and vs. vehicle mice were characterized by increased expression of *Hprt*, *Pmch*, *Gabre*, *Prlhr*, *Tox*, *Parpbb*, *Ngb*, *Gabrg3*, and *Galr1*. Administration of MPTP led to a decrease in *Arm4*, *Hsd17b7* expression and an increase in *Islr2*, *Tll3*, *Aldh3b2*, *Drc1* in groups of mice with MPTP vs. vehicle mice and MPTP+CBE vs. vehicle mice. Elevated *Prmt8* and *Ankrd63*

expression levels in mice with MPTP+CBE vs. CBE, vs. MPTP, vs. vehicle mice was found. In groups of mice with MPTP+CBE vs. MPTP and vs. vehicle mice, a decreased expression of *Sgk1* and *Arl4d* genes was observed, and in groups of mice with MPTP+CBE vs. CBE and vs. vehicle mice, two downregulated genes (*Slc24a2*, *Neto2*) and three upregulated genes (*Mef2c*, *Zfp831*, *Crocc*) were observed (Figure 2A). In groups of mice with MPTP vs. vehicle and mice with MPTP vs. mice with CBE, 11 common DEGs were found (*Hcrt*, *Pmch*, *Gabre*, *Prhr*, *Tox*, *Parpbp*, *Ngb*, *Gabrg3*, *Galr1*) (Table S7, Figure 2B).

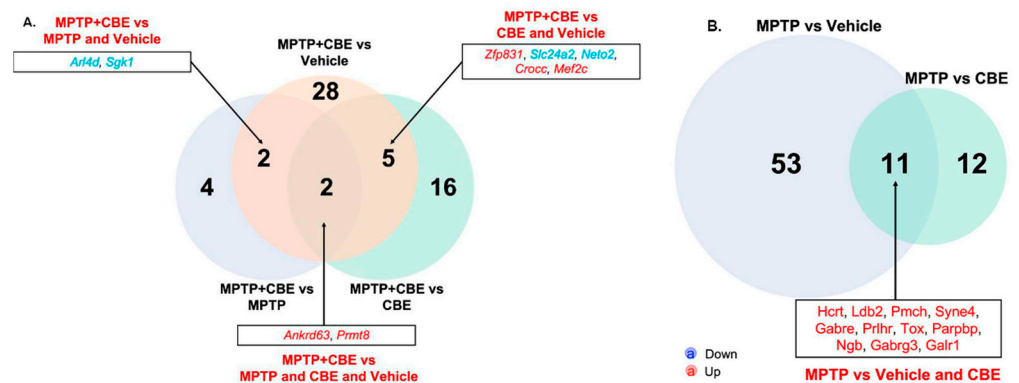


**Figure 2.** Venn Diagram of DEGs between the three studied groups of mice with (A) MPTP+CBE vs. CBE, MPTP+CBE vs. vehicle, MPTP+CBE vs. MPTP; (B) MPTP vs. vehicle, MPTP vs. CBE.

## 2.2. Gene Expression Outliers Highlight Targeted Pathways in Cojoined Influence of MPTP and CBE

Gene Ontology (GO) term enrichment analysis and gene set enrichment analysis (GSEA) were conducted for all determined DEGs. We considered “biological process” GO terms as well as all types of GO terms together (“biological process”, “molecular function”, “cellular component”) with a *p*-value (Bonferroni corrected) <0.05. All pathways determined with GSEA are shown in Figure 3. All pathways determined using GO analysis are shown in Figure 4. Using GSEA analysis, we found downregulated pathways associated with ion metabolism and upregulated pathways associated with neuronal function in MPTP+CBE mice vs. vehicle, upregulated pathways associated with inflammation and downregulated pathways associated with neuronal function in MPTP+CBE mice vs. MPTP mice and downregulated pathways associated with ion metabolism in MPTP+CBE mice vs. CBE mice (Figure 3). The alterations in pathways associated with neuronal function and inflammation were found using GO analysis in MPTP+CBE mice vs. vehicle and in MPTP+CBE mice vs. CBE and inflammation in MPTP+CBE vs. MPTP mice (Figure 4). Pronounced suppression of pathways associated with the endoplasmic reticulum (ER) was found in MPTP+CBE mice vs. vehicle using GSEA analysis with all types of GO terms (Figure 5). Mice with MPTP were characterized by pronounced alteration of ion metabolism and neuronal function compared to vehicle mice, and mice with MPTP were characterized by the disruption of apoptotic and inflammation pathways compared to CBE mice (Figures 3 and 4).

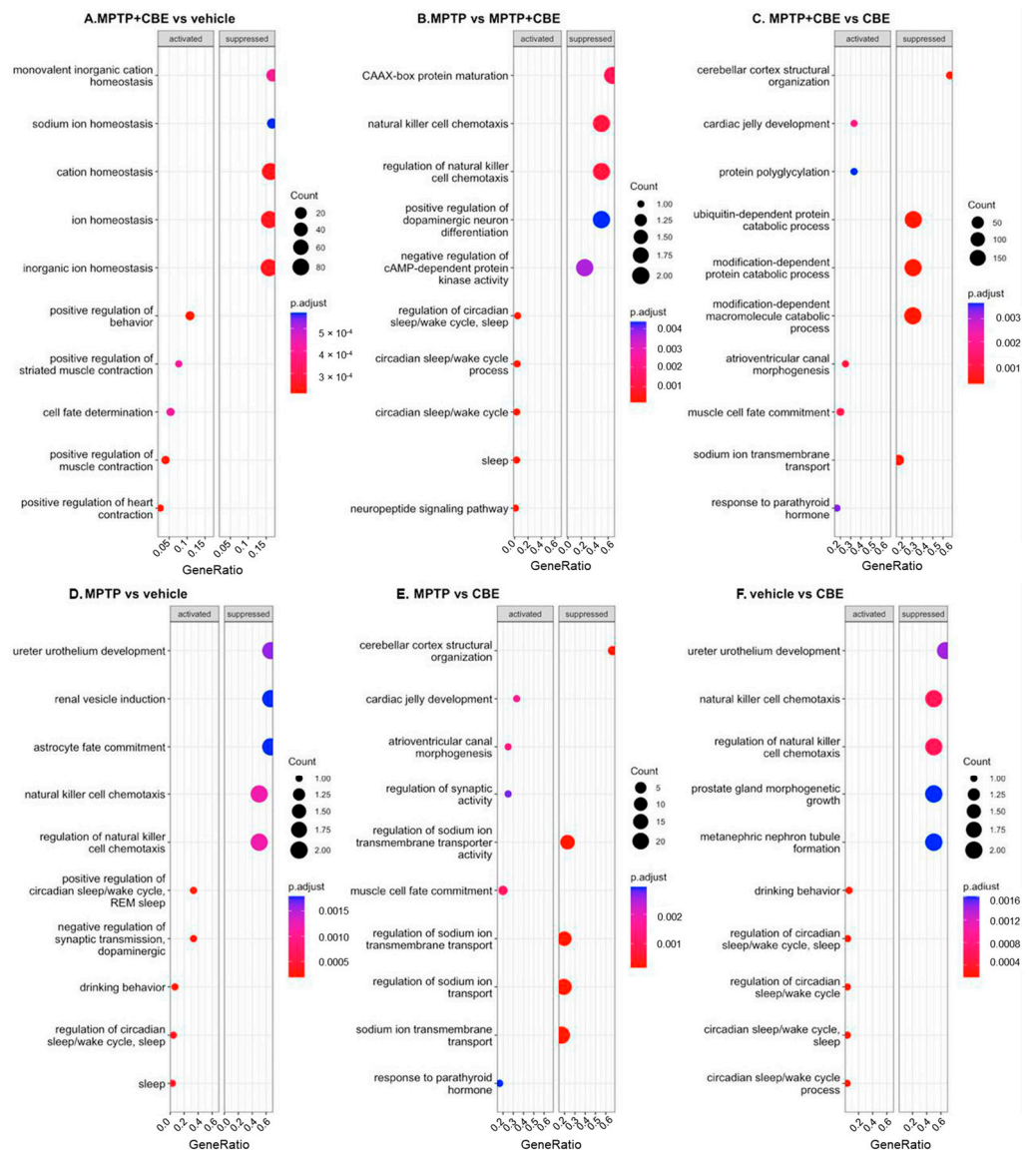


**Figure 3.** Enriched Biological Process GO terms: dot plot. The 10 GO processes with the largest gene ratios are plotted in order of gene ratio. (A) MPTP+CBE mice vs. vehicle, (B) MPTP+CBE mice vs. CBE mice, (C) MPTP mice vs. MPTP+CBE mice, (D) MPTP+CBE mice vs. vehicle, (E) MPTP+CBE mice vs. CBE mice, (F) MPTP mice vs. MPTP+CBE mice. The size of the dots represents the number of DEGs associated with the GO term, and the color of the dots represent the P-adjusted values.

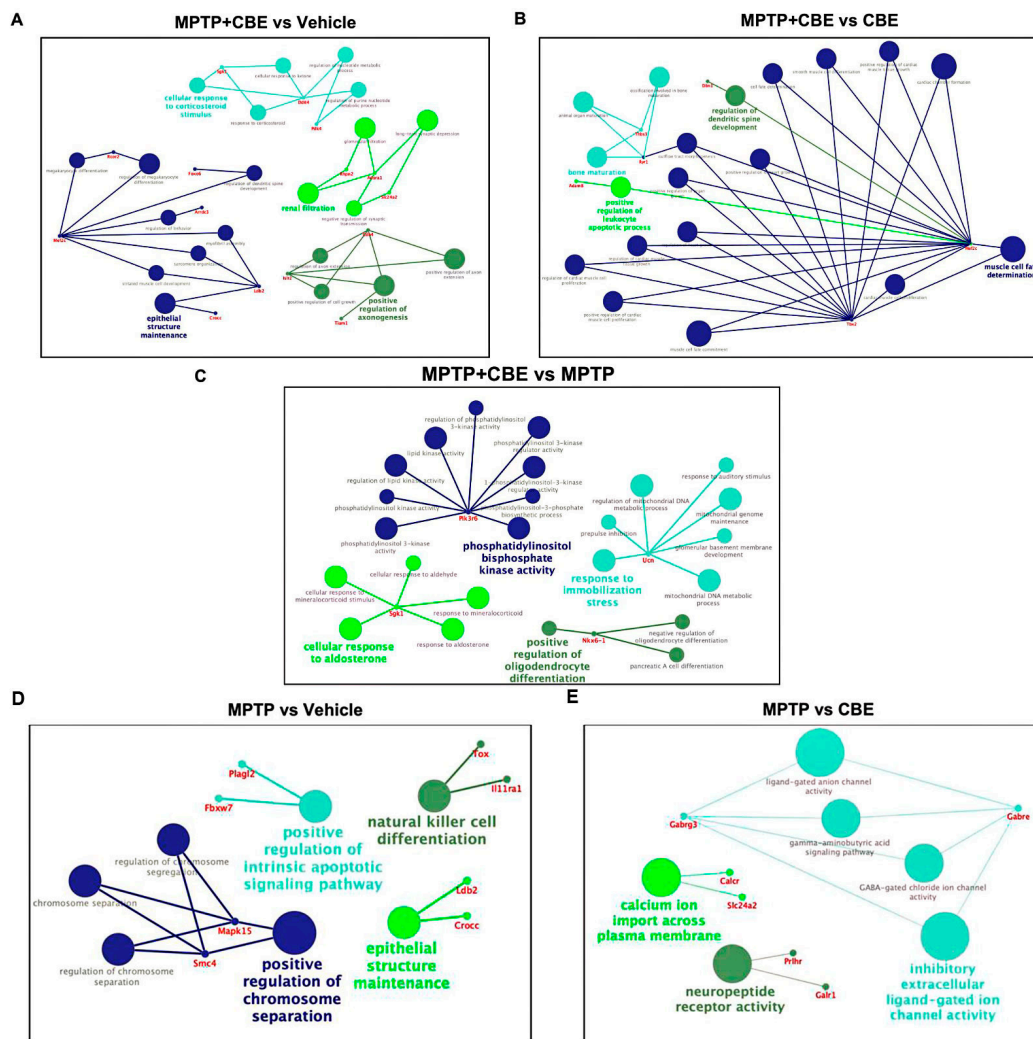


**Figure 4.** Networks of selected metabolic processes and DEGs in (A) MPTP+CBE mice vs. vehicle, (B) MPTP+CBE mice vs. CBE mice, (C) MPTP+CBE mice vs. MPTP mice, (D) MPTP mice vs. vehicle, (E) MPTP mice vs. CBE mice (obtained using CluePedia v. 1.5.9 + ClueGo v. 2.5.9).

### 2.3. Overlapping Analysis of Enriched Pathways in MPTP-CBE Mice Model and Data Set of RNA-Seq Peripheral Blood Monocyte-Derived Macrophages from L444P/N GBA-PD Patients

Raw data from our previous study comprised RNA-seq of peripheral blood monocyte-derived macrophages from L444P/N GBA-PD patients, asymptomatic *GBA1* mutation carriers (GBA carriers) and controls that had been deposited in NCBI's Gene Expression Omnibus [26] and are accessible through GEO Series accession number GSE184956 (<https://www.ncbi.nlm.nih.gov/geo/query/acc.cgi?acc=GSE184956> (accessed on 9 September 2021)). DEGs of compared groups are presented in Supplementary Tables S2–S4 of our previous article [12].

Next, we focused on top genes determined in the DEGs dataset of mice with MPTP+CBE vs. vehicle mice and the DEGs dataset of macrophages of L444P/N GBA-PD patients vs. controls [12]. Based on the literature and the website GeneCards (<https://www.genecards.org>, accessed on 1 June 2023), the products of the most of top genes of the two datasets are involved in the PI3K-Akt-mTOR pathway (Figure 6, Tables S8 and S9). Moreover, the genes from one ARL4 family (ADP ribosylation factor like GTPase 4) were present in the top list of the two datasets (*Arl4d*, *ARL4C*).

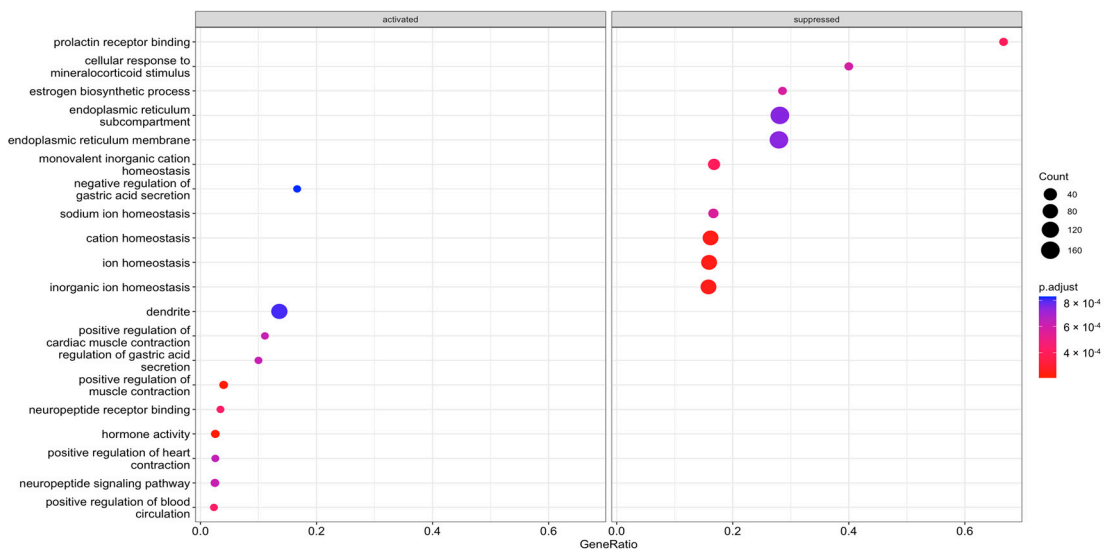


**Figure 5.** All enriched GO terms: dot plot. The 20 GO processes with the largest gene ratios are plotted in order of gene ratio in MPTP+CBE mice vs. vehicle. The size of the dots represents the number of DEGs associated with the GO term, and the color of the dots represent the P-adjusted values.

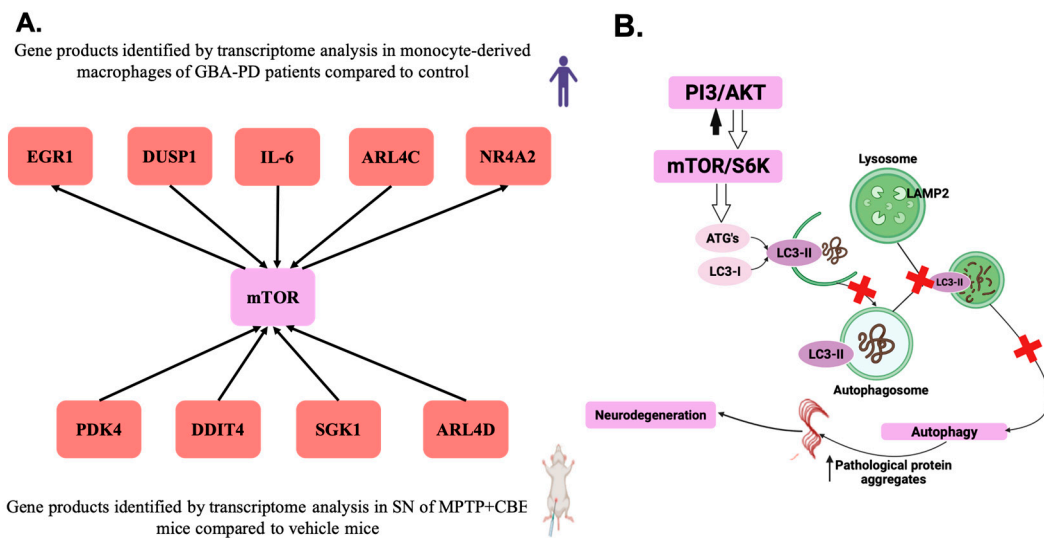


**Figure 6.** PI3K-Akt-mTOR pathway. **(A)** DEGs identified during the analysis of the top 10 DEGs in two datasets: monocyte-derived macrophages from patients with L444P/N GBA-PD compared to control and SNs MPTP+CBE mice and vehicle; **(B)** Schematic representation of the role of the PI3K-Akt-mTOR pathway in neurodegeneration—the mTOR complex mTORC1 acts upstream of the autophagic pathway to suppress autophagic membrane formation. Alteration of mTOR activity leads to disruption of autophagosome formation due to the suppressed kinase activity of cytosolic Atg proteins and, as a consequence, impairment of conjugation of LC3-I to PE for formation of LC3-II. LC3-II proteins then specifically associate with a newly formed crescent-shaped membrane termed a phagophore. Next, the phagophore is unable to elongate around cytosolic contents until the contents are completely sequestered within a fully formed double-membraned autophagosome. The mature autophagosomes cannot become acidic and fuse with lysosomes to form the degradative autolysosome. There is a violation of the process of autophagy and, as a result, a violation of the degradation of proteins, in particular, the alpha-synuclein protein, which possibly leads to neurodegeneration.

### 3. Discussion

The whole transcriptome analysis of cells from the SN of a mouse model of PD bearing defective GCase activity (double neurotoxic MPTP+CBE model) compared to vehicle mice was conducted for the first time. DEGs of CBE-treated and MPTP-treated mice were also analyzed.

In MPTP-treated animals, we revealed the disruption of pathways associated with neuronal function, apoptosis, vesicular transport and immune response (Figures 3 and 4). Thus, in some ways, we replicated the analysis conducted by Alieva and colleagues, who studied the transcriptome profile of SN in the MPTP-induced early stage of PD [27,28]. These authors found a dysregulation of pathways involved in vesicular transport and also in mitochondrial function, apoptosis, ubiquitin-dependent proteolysis, RNA splicing and myelination.

As for CBE-treated mice, Vardi and coauthors previously used CBE for the development of symptoms associated with neurological forms of GD and remarked on the similarities in the gene expression profiles in brain samples of CBE-treated mice and a genetic GD mouse model ( $Gba^{fllox/fllox}$ ; nestin-Cre mice) [28]. The authors suggested that CBE injection may provide a rapid and relatively easy way to induce symptoms typical of neuronal forms of GD [29]. A recent study found an alteration of expression in genes involved in the IFN response in brain samples of CBE-treated mice [30]. These data supported a previous study that demonstrated an activation of inflammation processes in liver and lung samples of *Gba1* point-mutated mice (V394L/V394L and D409V/null) [31]. Additionally, a recent study based on single cell transcriptome analysis of brain samples of GD model mice ( $Gba^{lnl/lnl}$  mice with 134 germ-line deletion of *Gba*) found activation of neuroinflammation in the form of attrition of homeostatic microglia, emergence of DAM, influx of CCR2+ MFs, activation of the ISG pathway and infiltration of activated NK cells [32]. We found one downregulated DEG, *Pomc*, in CBE-treated mice (Table S6). The product of this gene, the precursor protein proopiomelanocortin, plays multiple roles in the cell, such as stress response, immune system, the central melanocortin system and regulating feeding behavior [33]. GSEA analysis revealed the alteration of pathways associated with inflammation (Figure 3). Downregulated expression of *Pomc* may be associated with inflammation in response to CBE injection.

Our previous study performed unbiased transcriptomic analysis of monocyte-derived macrophages comparing GBA-PD and non-manifesting GBA carriers and control subjects [12]. We found an aberration of immune response, neuronal function and zinc metabolism pathways in GBA-PD and GBA carriers and more pronounced altered expression of genes involved in autophagy in GBA-PD patients than in GBA carriers [12]. Another study, using gene-based outlier analysis, found the disruption of lysosomal, membrane trafficking, and mitochondrial processing in circulating monocytes CD14+ of GBA-PD patients compared to GBA carriers [34].

Here, we focused on the analysis of MPTP+CBE-treated mice vs. vehicle mice. We revealed 8 DEGs in mice with MPTP+CBE vs. MPTP (6 upregulated DEGs, 2 downregulated DEGs), 23 DEGs in mice with MPTP+CBE vs. CBE (16 upregulated DEGs, 7 downregulated DEGs) and 37 DEGs in mice with MPTP+CBE vs. vehicle mice (21 upregulated DEGs, 16 downregulated DEGs). Following the GSEA analysis, we found upregulated pathways associated with neuronal processes and downregulated pathways associated with ion metabolism. Following the GO analysis, the alteration of inflammation processes was found (Figures 3 and 4). The revealed upregulated neuronal activity may be associated with induced processes of neurodegeneration, which is supported by a decrease in dopamine level in the striatum of mice with MPTP+CBE compared to vehicle mice [25]. The disruption of ion metabolism may be also associated with the involvement of several ion channels in the release of dopamine in SN neurons. An earlier study reported that ion channels play a central role in driving the high vulnerability of dopaminergic neurons to degeneration during PD [35]. Dysregulation of ion channels causes the aberrant movement of various ions in the intracellular milieu, which leads to the disruption of intracellular signaling



cascades, alterations in cellular homeostasis, and bioenergetic deficits [35,36]. It is well known that *GBA1* mutations lead to increased secretion of proinflammatory cytokines. In our previous study, we reported increased proinflammatory cytokines in the plasma of GBA-PD patients [37]. Mice with p.Asp409Val/knockout in *GBA1* had increased levels of inflammatory cells and cytokines including IFN $\gamma$ , TNF, IL-1 $\beta$ , IL-6, and IL-17A/E, as well [38]. Another study demonstrated that glucosylceramide, one of the main substrates of GCase, can activate myeloid cells and increase the levels of inflammatory cytokines in the thymus of hematopoietic-specific *GBA1*-deficient mice [39].

Enriched all GO terms analysis additionally revealed pronounced suppression of ER pathways in MPTP+CBE mice (Figure 5). ER plays a key role in the synthesis, glycosylation and folding of proteins [40], and ER stress leads to the accumulation of unfolded or misfolded proteins. Several reviews have discussed how ER stress is a causative factor in PD [41,42]. *GBA1* mutations may lead to the production of a misfolded protein, which can be retained in the ER to induce ER stress [43]. As Maor and colleagues demonstrated, *GBA1* mutations lead to their retention in the ER and subsequent activation of the UPR (unfolded protein response) in the *Drosophila* model [44]. Post-mortem analysis of brains of Lewy bodies dementia (LDB) patients carrying *GBA1* mutations showed an abnormal UPR response that was associated with ER stress [45]. All of these observations in a model with GCase dysfunction were accompanied by an increased  $\alpha$ -synuclein level that proved the link between ER stress and  $\alpha$ -synuclein metabolism [46–48]. Our mice model with MPTP+CBE was also characterized by an increased  $\alpha$ -synuclein level in the striatum [25], along with downregulated ER activity followed by GSEA analysis (Figure 5), which supports previous results. Kuo and colleagues suggested that GCase that fails to fold in the ER is efficiently targeted to lysosomes by chaperone-mediated autophagy (CMA), but blocks the multimerization of LAMP2A, resulting in a disruption of proteostasis and  $\alpha$ -synuclein accumulation [49]. In our previous study, we found a decrease in expression of the *LAMP2* gene in CD45+ blood cells in GBA-PD and PD patients compared to controls, with a more pronounced decrease in *LAMP2* expression in GBA-PD, supporting the role of the disruption of the autophagy–lysosome pathway in GCase dysfunction [50].

Next, we focused on the top ten DEGs in comparative groups of MPTP-CBE mice vs. vehicle mice and compared them with the top ten from the dataset of DEGs revealed during our previous research conducted on peripheral blood monocyte-derived macrophages from L444P/N GBA-PD patients [12]. The products of the top DEGs in MPTP+CBE vs. vehicle mice appeared to be involved in the PI3K-Akt-mTOR pathway (Figure 6). It is interesting that similar alterations of this pathways were determined in peripheral blood monocyte-derived macrophages from L444P/N GBA-PD patients (Figure 6). The PI3K/AKT/mTOR pathway regulates autophagy, apoptosis, cell cycle, inflammation, and according to the previous data, may be involved in neurodegeneration [51,52].

In our current study, MPTP+CBE mice were characterized by decreased expression of *Sgk1*, *Pdk4*, *Arl4d*, *Arrdc3*, and *Ddit4*. The *Sgk1* gene encodes serum- and glucocorticoid-dependent kinase 1 (SGK1). Earlier, a downregulated level of *Sgk1* was reported in SNs of mice with chronic MPTP intoxication [53]. Pyruvate dehydrogenase kinase (PDK) is also located in the outer mitochondrial membrane and can negatively regulate PDH activity by phosphorylating one of its subunits. Early overexpression of PDK4 may protect cells from damage caused by ROS, and attenuate neuronal apoptosis by reducing oxidative stress [54,55]. The PI3K/AKT/mTOR pathway affects the oxidative stress pathway through other downstream signaling molecules, such as FoxO3a, in addition to GSK-3beta, to influence PD [56]. We found an increased expression of Foxo6 in MPTP+CBE mice (Figure 1, Table S2). Members of the FoxO subfamily shuttle from the cytoplasm to the nucleus and play an important role in cell proliferation, apoptosis, differentiation and oxidative stress resistance. It was hypothesized that SGK1 may play a critical role downstream of PDK1 in sustaining mTORC1 activity [57]. mTORC1 activity was augmented with PDK4 overexpression and reduced by PDK4 suppression in various cell lines [58]. The coding product of the *DDIT4* gene is a stress-induced protein called RTP801/REDD1 [59]. RTP801

is a negative regulator of mTOR [60,61]. RTP801/REDD1 inhibits the activity of mTOR and participates in the regulation of diverse cell functions including proliferation, apoptosis and differentiation. RTP801 was elevated in the SN of PD patients [61]. Here, we found downregulated *Ddit4* expression in MPTP+CBE mice vs. vehicle, which may be associated with activation of mTOR activity. A recent study also demonstrated decreased *Ddit4* in a mouse model with chronic MPTP treatment after 14 days compared to vehicle [62]. ARL4D, ARL4A and ARL4C are closely related members of the ADP-ribosylation factor/ARF-like protein (ARF/ARL) family of GTPases. ARL4D is located primarily at the plasma membrane, but can also be detected in the nucleus and cytoplasm. Dysfunctional GTP-binding-defective ARL4D is targeted to mitochondria functions, vesicular transport [63]. Interestingly, common family genes were found when comparing the two data sets (peripheral blood mononuclear cells (PBMC)-derived macrophages and SN of mice). There were two genes (*ARL4C* and *Alr4d*) encoding the proteins from Arl4 family (ADP ribosylation factor (Arf)-like 4 proteins). *ARL4C* and *Alr4d* are involved in the PI3K/AKT/mTOR pathway [64].

When comparing datasets of DEGs in MPTP+CBE mice to MPTP mice, CBE mice and vehicle mice, two DEGs (*Ankrd63*, a gene with products without well-established function, and *Prmt8*, which regulates the maturation of synapses and neural circuits during brain development [65]) were identified. As expected, five common DEGs in MPTP+CBE mice compared to CBE mice and vehicle mice were involved in neurogenesis and dopamine transport (*Zfp831*, *Slc24a2*, *Neto2*, *Crocc*, *Mef2c*), thus suggesting a potentiating effect of MPTP on alteration of neuronal function (Figure 2). Two common DEGs (*Arl4d*, *Sgk1*) were identified in MPTP+CBE mice compared to MPTP mice and vehicle mice. They are involved in the PI3K-Akt-mTOR pathway, thus suggesting a potentiating effect of CBE and, as a consequence of GCase dysfunction, an effect on the disruption of autophagy processes (Figure 2). Interestingly, monocyte-derived macrophages of patients with L444P/N GBA-PD were also characterized by a more pronounced change in the genes involved in the PI3K-Akt-mTOR pathway compared to L444P/N GBA carriers and controls (*DUSP1*, *ARL4C*) (Table S9) [12].

We found a similar alteration in the PI3K-Akt-mTOR pathway in condition of GCase dysfunction in our PD models, both in primary macrophages from patients with GBA-PD and in the double toxic model MPTP+CBE-treated mice (Figure 6B). Recently, disturbances in the autophagy-lysosomal pathway, which co-occur with upstream perturbations in mTOR activation, were found using proteome analysis of induced pluripotent stem cell (iPSC) dopamine neurons of GBA-PD patients [66]. Additionally, single-cell RNA sequencing and proteomics of brain samples from GBA-PD patients confirmed reduced CMA activity and proteome changes comparable to those found in brain samples from heterozygous L444P/N *GBA1* mice [49]. Interestingly, glycoproteome analysis revealed a number of significantly enriched pathways, including ceramide catabolic processes, and also an increased level of glycosylated LAMP1, LAMP2 and cathepsin D, which are necessary for transport from the ER via the Golgi to the lysosome, in GBA-PD iPSC-dopamine neurons. Increased phosphorylated mTOR level was supported with Western blot analysis [66]. Earlier, we found differences in lysosomal hydrolase activity (alpha-galactosidase (GLA), alpha-iduronidase (IDUA)) in iPSC neurons of GBA-PD compared to GBA carriers, suggesting that a more pronounced imbalance of sphingolipid metabolism may lead to impaired lysosomal clearance and launch the diseases associated with GCase deficiency [67]. Moreover, treatment with a compound (Genz-123346) that inhibits glycosphingolipid biosynthesis decreases mTOR activity and restores TFEB expression in GBA-PD iPSC neurons, demonstrating a possible link between mTOR-TFEB alterations and lipid accumulation [68]. Inhibition of mTOR by selective inhibitors restored TFEB activity, which plays a role in the regulation of lysosomal biogenesis and autophagy, decreased ER stress and reduced alpha-synuclein protein level, suggesting the improvement of neuronal proteostasis on GBA-PD iPSC neurons [68]. However, it is still necessary to look for what distinguishes

between GBA-PD and GBA carriers, as the penetrance of heterozygous *GBA1* mutations for PD is variable from 10% to 30% [69].

Taken together, our data support dysfunction of the autophagy–lysosomal pathway as a central pathogenic event in GBA-associated neurodegenerative disease, as has been suggested [70,71]. Although autophagic disturbances were also revealed in MPTP-treated mice with targeted or whole transcriptomic approaches including our previous study [72–75], our findings demonstrated a more pronounced change in the PI3K-Akt-mTOR pathway in the case of GCase deficiency.

The current study has some limitations. The small size of the studied groups of mice may influence the outcome of differential expression analysis for genes with small differences in expression levels, eliminating nonspecific gene expression differences.

## 4. Materials and Methods

### 4.1. Brain Samples from Mice

Sixteen mice C57BL/6 8–12 weeks old weighing 22–26 g were generated and separated into four groups with four animals in each, and treated with the following solutions: 0.9% sodium chloride solution (vehicle mice), conduritol  $\beta$ -epoxide (CBE) with MPTP (MPTP-CBE), CBE, MPTP. The animals were maintained at 21–23 °C in a 12 h light/dark cycle having free access to food and tap water. In the CBE group, CBE was intraperitoneally injected once in an individual dose of 100 mg/kg. In the MPTP group, MPTP was subcutaneously injected twice, with 2 h intervals between the injections, at the individual dose of 12 mg/kg, as described earlier by Ugrumov et al. [24]. In the MPTP+CBE group, MPTP was subcutaneously injected twice with 2 h intervals between the injections at the individual dose of 12 mg/kg, and CBE was injected intraperitoneally once with an individual dose of 100 mg/kg simultaneously with the second injection of MPTP. To assess motor dysfunction, the “Grip strength” (GRIP-test) [76] and “Open field” behavioral tests [77] were carried out 2 weeks after injections. Animals were sacrificed 2 weeks after injection day. The brain samples were removed from the skull and cut along the midsagittal plane. The substantia nigra was dissected under a dissecting microscope with an ocular micrometer (Nikon SMZ660, Nikon, Melville, NY, USA). Samples of peripheral blood were obtained from all animals. SN samples were obtained and frozen and kept at –70 °C until RNA isolation.

### 4.2. RNA Isolation and RNA Sequencing (RNA-Seq)

Whole-transcriptome analysis was performed using pooled brain tissues of SN of mice with MPTP-CBE-induced PD with GCase dysfunction, MPTP-induced PD, CBE and control mice (vehicle) with NaCl. For this purpose, 5 mg of brain tissue was taken from each of the four animals in each group. Total RNA was extracted from brain tissue with Trisol reagent and PureLink RNA micro Kit (PureLink RNA micro Kit, Invitrogen, CA, USA), according to the manufacturer’s instruction. The quality was checked with a BioAnalyser (2100 Bioanalyzer Instrument, Agilent, CA, USA) and RNA 6000 Nano Kit (RNA 6000 Nano Kit, Agilent, CA, USA). PolyA RNA was purified with Dynabeads<sup>®</sup> mRNA Purification Kit (Dynabeads<sup>®</sup> mRNA Purification Kit, Ambion, TX, USA). The Illumina library was made from polyA NEBNext<sup>®</sup> Ultra<sup>™</sup> II RNA Library Prep (NEBNext<sup>®</sup> Ultra<sup>™</sup> II RNA Library Prep, NEB, MA, USA), according to the manual. Sequencing was performed on a HiSeq1500 (Illumina, CA, USA) with 50 bp read length. At least ten million reads were generated for each sample.

### 4.3. Quality Control

Quality control for each sample was performed using FastQC (v0.11.9) [78] and RSeQC (v4.0.0) [79]. In this step, clean data (clean reads) were obtained by removing low-quality reads, reads containing adapters, and reads containing ploy-N from raw data. The removal adapter was conducted with Cutadapt [80]. All downstream analyses were based on clean data.

#### 4.4. Reads Mapping to Reference Genome

Mouse reference genome assembly GRCm39 and gene model annotation files were downloaded from the Gencode website (<https://www.gencodegenes.org/mouse/> (accessed on 28 March 2023)) directly (release M32). HISAT2 (v2.2.1) [81] was used with default parameters to build the index of the reference genome and to map reads to the genome.

#### 4.5. Quantification of Gene Expression Level

Counting of sequencing reads mapping to each gene after the alignment step was performed using the HTSeq-count function from the HTSeq framework (v.0.6.1) [82].

#### 4.6. Analysis of Gene Differential Expression

Gene differential expression analyses of the three groups were performed using the DESeq2 package (v.1.30.1) [83] in R (v.4.1.2). DESeq2 provides statistical routines for determining differential expression in digital gene expression data using a model based on negative binomial distribution. The resulting *p*-values were adjusted using Benjamini and Hochberg's approach for controlling the false discovery rate (FDR). The groups of mice were subdivided into subgroups based on the symptomatic (mice with MPTP vs. NaCl (vehicle mice)) and GCase dysfunction (mice with MPTP-CBE, mice with CBE and mice without GCase dysfunction (MPTP, NaCl/vehicle)). Results from the comparison of each pair of groups were then extracted. A threshold of FDR < 0.05 was utilized as the threshold of significance. Detected differential expression of genes was considered statistically significant at *p*-value  $\leq 0.01$  and a fold change (FC) threshold > 1.5. The differentially expressed genes were visualized in a volcano plot built using ggplot (v.3.3.3) in R (v 4.0.3).

#### 4.7. GO Enrichment Analysis of Differentially Expressed Genes

GO enrichment analysis of differentially expressed genes was performed using the GO resource (<http://geneontology.org> (accessed on March 2023)) and was carried out using the apps ClueGO v. 2.5.7 [84] and CluePedia v. 1.5.3 [85] for Cytoscape v. 3.6.1. GO terms with a corrected *p*-value of less than 0.05 were considered. Term groups were selected using ClueGO based on the number of common genes/terms (>50%). Term clusters were selected based on common genes. Functional clustering and annotation of selected genes were performed using the STRING database (version 10.0). Venn diagrams were constructed in the VennDiagram software package for R (version 3.4.0). A corrected *p* value (Benjamini) was calculated for each functional cluster.

## 5. Conclusions

We identified a set of genes and molecular pathways that are specific to PD with GCase dysfunction in the SN of mice treated with co-injection of MPTP and CBE. These genes and pathways related to dysregulation of lysosomal, membrane trafficking, inflammation and mitochondrial processes, suggesting that alteration of these processes is more pronounced in samples manifesting GBA-PD. We found a common altered PI3K-Akt-mTOR signaling pathway that regulates key process in GBA-PD pathogenesis, such as autophagy and immune response based on comparative analysis of transcriptomic data of human monocyte-derived macrophages and SN cells of mice with PD and GCase dysfunction. Further investigation will clarify the possible role as PD biomarkers of these hits.

**Supplementary Materials:** The following supporting information can be downloaded at: <https://www.mdpi.com/article/10.3390/ijms241512164/s1>. References [64,86–93] are cited in the supplementary materials.

**Author Contributions:** T.U.: writing—original draft, formal analysis, visualization, investigation, A.B.: formal analysis, visualization, investigation, M.M.R.: investigation, K.B.: investigation, M.I.S.: investigation, E.Z.: investigation, P.A.S.: investigation, S.P.: conceptualization, resources, funding acquisition, supervision, writing—review and editing. All authors have read and agreed to the published version of the manuscript.

**Funding:** This research was funded by the Russian Science Foundation Grant No. 19-15-00315 in part of generation of mouse models, and by the Ministry of Science and Higher Education of the Russian Federation Project No 121060200125-2, “The study of molecular and cellular components of the pathogenesis of socially significant diseases for the development of methods for early diagnosis and treatment” in part of bioinformatic analysis.

**Institutional Review Board Statement:** Experiments with laboratory animals were performed in accordance with The Guide for the Care and Use of Laboratory Animals. The study was approved by the Ethics Committee of the Institute of Molecular Genetics of Russian Academy of Sciences.

**Informed Consent Statement:** Not applicable.

**Data Availability Statement:** The data discussed in this publication have been deposited at ArrayExpress database at EMBL-EBI (<https://www.ebi.ac.uk/biostudies/> (accessed on 25 July 2023)) under accession number S-BSST1159 <https://www.ebi.ac.uk/biostudies/studies/S-BSST1159> (accessed on 25 July 2023) for array design “S-BSST1159”.

**Conflicts of Interest:** The authors declare no conflict of interest.

## References

1. Lee, V.M.-Y.; Trojanowski, J.Q. Mechanisms of Parkinson’s Disease Linked to Pathological  $\alpha$ -Synuclein: New Targets for Drug Discovery. *Neuron* **2006**, *52*, 33–38. [[CrossRef](#)]
2. Xu, L.; Pu, J. Alpha-Synuclein in Parkinson’s Disease: From Pathogenetic Dysfunction to Potential Clinical Application. *Park. Dis.* **2016**, *2016*, 1720621. [[CrossRef](#)]
3. Gan-Or, Z.; Giladi, N.; Rozovski, U.; Shifrin, C.; Rosner, M.S.; Gurevich, T.; Bar-Shira, A.; Orr-Urtreger, A. Genotype-Phenotype Correlations between GBA Mutations and Parkinson Disease Risk and Onset. *Neurology* **2008**, *70*, 2277–2283. [[CrossRef](#)] [[PubMed](#)]
4. Lesage, S.; Anheim, M.; Condroyer, C.; Pollak, P.; Durif, F.; Dupuits, C.; Viallet, F.; Lohmann, E.; Corvol, J.-C.; Honoré, A.; et al. Large-Scale Screening of the Gaucher’s Disease-Related Glucocerebrosidase Gene in Europeans with Parkinson’s Disease. *Hum. Mol. Genet.* **2011**, *20*, 202–210. [[CrossRef](#)] [[PubMed](#)]
5. Li, Y.; Sekine, T.; Funayama, M.; Li, L.; Yoshino, H.; Nishioka, K.; Tomiyama, H.; Hattori, N. Clinicogenetic Study of GBA Mutations in Patients with Familial Parkinson’s Disease. *Neurobiol. Aging* **2014**, *35*, 935.e3–935.e8. [[CrossRef](#)] [[PubMed](#)]
6. Sidransky, E.; Nalls, M.A.; Aasly, J.O.; Aharon-Peretz, J.; Annesi, G.; Barbosa, E.R.; Bar-Shira, A.; Berg, D.; Bras, J.; Brice, A.; et al. Multicenter Analysis of Glucocerebrosidase Mutations in Parkinson’s Disease. *N. Engl. J. Med.* **2009**, *361*, 1651–1661. [[CrossRef](#)] [[PubMed](#)]
7. Emelyanov, A.K.; Usenko, T.S.; Tesson, C.; Senkevich, K.A.; Nikolaev, M.A.; Miliukhina, I.V.; Kopytova, A.E.; Timofeeva, A.A.; Yakimovsky, A.F.; Lesage, S.; et al. Mutation Analysis of Parkinson’s Disease Genes in a Russian Data Set. *Neurobiol. Aging* **2018**, *71*, 267.e7–267.e10. [[CrossRef](#)] [[PubMed](#)]
8. Aflaki, E.; Stubblefield, B.K.; Maniawang, E.; Lopez, G.; Moaven, N.; Goldin, E.; Marugan, J.; Patnaik, S.; Dutra, A.; Southall, N.; et al. Macrophage Models of Gaucher Disease for Evaluating Disease Pathogenesis and Candidate Drugs. *Sci. Transl. Med.* **2014**, *6*, 240ra73. [[CrossRef](#)] [[PubMed](#)]
9. Pant, D.C.; Aguilera-Albesa, S.; Pujol, A. Ceramide Signalling in Inherited and Multifactorial Brain Metabolic Diseases. *Neurobiol. Dis.* **2020**, *143*, 105014. [[CrossRef](#)]
10. Lai, M.; La Rocca, V.; Amato, R.; Freer, G.; Pistello, M. Sphingolipid/Ceramide Pathways and Autophagy in the Onset and Progression of Melanoma: Novel Therapeutic Targets and Opportunities. *Int. J. Mol. Sci.* **2019**, *20*, 3436. [[CrossRef](#)]
11. Sabrin, A.; Stiban, J. Roles of Ceramides and Other Sphingolipids in Immune Cell Function and Inflammation. In *The Role of Bioactive Lipids in Cancer, Inflammation and Related Diseases*; Honn, K.V., Zeldin, D.C., Eds.; Springer International Publishing: Cham, Switzerland, 2019; pp. 169–191. ISBN 978-3-030-21735-8.
12. Usenko, T.; Bezrukova, A.; Basharova, K.; Panteleeva, A.; Nikolaev, M.; Kopytova, A.; Miliukhina, I.; Emelyanov, A.; Zakharova, E.; Pchelina, S. Comparative Transcriptome Analysis in Monocyte-Derived Macrophages of Asymptomatic GBA Mutation Carriers and Patients with GBA-Associated Parkinson’s Disease. *Genes* **2021**, *12*, 1545. [[CrossRef](#)]
13. Alcalay, R.N.; Levy, O.A.; Waters, C.C.; Fahn, S.; Ford, B.; Kuo, S.H.; Mazzoni, P.; Pauciuolo, M.W.; Nichols, W.C.; Gan-Or, Z.; et al. Glucocerebrosidase Activity in Parkinson’s Disease with and without GBA Mutations. *Brain* **2015**, *138*, 2648–2658. [[CrossRef](#)]
14. Guedes, L.C.; Chan, R.B.; Gomes, M.A.; Conceição, V.A.; Machado, R.B.; Soares, T.; Xu, Y.; Gaspar, P.; Carriço, J.A.; Alcalay, R.N.; et al. Serum Lipid Alterations in GBA-Associated Parkinson’s Disease. *Park. Relat. Disord.* **2017**, *44*, 58–65. [[CrossRef](#)]

15. Pchelina, S.; Emelyanov, A.; Baydakova, G.; Andoskin, P.; Senkevich, K.; Nikolaev, M.; Miliukhina, I.; Yakimovskii, A.; Timofeeva, A.; Fedotova, E.; et al. Oligomeric  $\alpha$ -Synuclein and Glucocerebrosidase Activity Levels in GBA-Associated Parkinson's Disease. *Neurosci. Lett.* **2017**, *636*, 70–76. [[CrossRef](#)] [[PubMed](#)]
16. Pchelina, S.; Baydakova, G.; Nikolaev, M.; Senkevich, K.; Emelyanov, A.; Kopytova, A.; Miliukhina, I.; Yakimovskii, A.; Timofeeva, A.; Berkovich, O.; et al. Blood Lysosphingolipids Accumulation in Patients with Parkinson's Disease with Glucocerebrosidase 1 Mutations. *Mov. Disord.* **2018**, *33*, 1325–1330. [[CrossRef](#)] [[PubMed](#)]
17. Kopytova, A.E.; Usenko, T.S.; Baydakova, G.V.; Nikolaev, M.A.; Senkevich, K.A.; Izyumchenko, A.D.; Tyurin, A.A.; Miliukhina, I.V.; Emelyanov, A.K.; Zakharova, E.Y.; et al. Could Blood Hexosylsphingosine Be a Marker for Parkinson's Disease Linked with GBA1 Mutations? *Mov. Disord.* **2022**, *37*, 1779–1781. [[CrossRef](#)] [[PubMed](#)]
18. Langston, J.W.; Ballard, P.; Tetrud, J.W.; Irwin, I. Chronic Parkinsonism in Humans Due to a Product of Meperidine-Analog Synthesis. *Science* **1983**, *219*, 979–980. [[CrossRef](#)] [[PubMed](#)]
19. Muñoz-Manchado, A.B.; Villadiego, J.; Romo-Madero, S.; Suárez-Luna, N.; Bermejo-Navas, A.; Rodríguez-Gómez, J.A.; Garrido-Gil, P.; Labandeira-García, J.L.; Echevarría, M.; López-Barneo, J.; et al. Chronic and Progressive Parkinson's Disease MPTP Model in Adult and Aged Mice. *J. Neurochem.* **2016**, *136*, 373–387. [[CrossRef](#)]
20. Mustapha, M.; Mat Taib, C.N. MPTP-Induced Mouse Model of Parkinson's Disease: A Promising Direction of Therapeutic Strategies. *Biomol. Biomed.* **2021**, *21*, 422–433. [[CrossRef](#)]
21. Meredith, G.; Rademacher, D. MPTP Mouse Models of Parkinson's Disease: An Update. *J. Park. Dis.* **2011**, *1*, 19–33. [[CrossRef](#)]
22. Kanfer, J.N.; Legler, G.; Sullivan, J.; Raghavan, S.S.; Mumford, R.A. The Gaucher Mouse. *Biochem. Biophys. Res. Commun.* **1975**, *67*, 85–90. [[CrossRef](#)]
23. Mus, L.; Siani, F.; Giuliano, C.; Ghezzi, C.; Cerri, S.; Blandini, F. Development and Biochemical Characterization of a Mouse Model of Parkinson's Disease Bearing Defective Glucocerebrosidase Activity. *Neurobiol. Dis.* **2019**, *124*, 289–296. [[CrossRef](#)] [[PubMed](#)]
24. Ugrumov, M.V.; Khaindrava, V.G.; Kozina, E.A.; Kucheryanu, V.G.; Bocharov, E.V.; Kryzhanovsky, G.N.; Kudrin, V.S.; Narkevich, V.B.; Klodt, P.M.; Rayevsky, K.S.; et al. Modeling of Presymptomatic and Symptomatic Stages of Parkinsonism in Mice. *Neuroscience* **2011**, *181*, 175–188. [[CrossRef](#)] [[PubMed](#)]
25. Pchelina, S.N.; Bezrukova, A.I.; Rudenok, M.M.; Zhuravlev, A.S.; Rybolovlev, I.N.; Baydakova, G.V.; Nikolaev, M.A.; Nesterov, M.S.; Abaimov, D.A.; Usenko, T.S.; et al. Biochemical characterization of double toxic MPTP/CBE presymptomatic Parkinson like phenotype in mice. *NeuroToxicology* **2023**. *submitted*.
26. Edgar, R.; Domrachev, M.; Lash, A.E. Gene Expression Omnibus: NCBI Gene Expression and Hybridization Array Data Repository. *Nucleic Acids Res.* **2002**, *30*, 207–210. [[CrossRef](#)] [[PubMed](#)]
27. Alieva, A.K.; Filatova, E.V.; Kolacheva, A.A.; Rudenok, M.M.; Slominsky, P.A.; Ugrumov, M.V.; Shadrina, M.I. Transcriptome Profile Changes in Mice with MPTP-Induced Early Stages of Parkinson's Disease. *Mol. Neurobiol.* **2017**, *54*, 6775–6784. [[CrossRef](#)]
28. Alieva, A.K.; Zyrin, V.S.; Rudenok, M.M.; Kolacheva, A.A.; Shulskaya, M.V.; Ugrumov, M.V.; Slominsky, P.A.; Shadrina, M.I. Whole-Transcriptome Analysis of Mouse Models with MPTP-Induced Early Stages of Parkinson's Disease Reveals Stage-Specific Response of Transcriptome and a Possible Role of Myelin-Linked Genes in Neurodegeneration. *Mol. Neurobiol.* **2018**, *55*, 7229–7241. [[CrossRef](#)]
29. Vardi, A.; Zigdon, H.; Meshcheriakova, A.; Klein, A.D.; Yaacobi, C.; Eilam, R.; Kenwood, B.M.; Rahim, A.A.; Massaro, G.; Merrill, A.H., Jr.; et al. Delineating Pathological Pathways in a Chemically Induced Mouse Model of Gaucher Disease. *J. Pathol.* **2016**, *239*, 496–509. [[CrossRef](#)]
30. Vardi, A.; Ben-Dor, S.; Cho, S.M.; Kalinke, U.; Spanier, J.; Futerman, A.H. Mice Defective in Interferon Signaling Help Distinguish between Primary and Secondary Pathological Pathways in a Mouse Model of Neuronal Forms of Gaucher Disease. *J. Neuroinflammation* **2020**, *17*, 265. [[CrossRef](#)]
31. Xu, Y.-H.; Jia, L.; Quinn, B.; Zamzow, M.; Stringer, K.; Aronow, B.; Sun, Y.; Zhang, W.; Setchell, K.D.R.; Grabowski, G.A. Global Gene Expression Profile Progression in Gaucher Disease Mouse Models. *BMC Genom.* **2011**, *12*, 20. [[CrossRef](#)] [[PubMed](#)]
32. Boddupalli, C.S.; Nair, S.; Belinsky, G.; Gans, J.; Teeple, E.; Nguyen, T.-H.; Mehta, S.; Guo, L.; Kramer, M.L.; Ruan, J.; et al. Neuroinflammation in Neuronopathic Gaucher Disease: Role of Microglia and NK Cells, Biomarkers, and Response to Substrate Reduction Therapy. *Elife* **2022**, *11*, e79830. [[CrossRef](#)] [[PubMed](#)]
33. Millington, G.W.M. The Role of Proopiomelanocortin (POMC) Neurons in Feeding Behaviour. *Nutr. Metab.* **2007**, *4*, 18. [[CrossRef](#)] [[PubMed](#)]
34. Riboldi, G.M.; Vialle, R.A.; Navarro, E.; Udine, E.; de Paiva Lopes, K.; Humphrey, J.; Allan, A.; Parks, M.; Henderson, B.; Astudillo, K.; et al. Transcriptome Deregulation of Peripheral Monocytes and Whole Blood in GBA-Related Parkinson's Disease. *Mol. Neurodegener.* **2022**, *17*, 52. [[CrossRef](#)] [[PubMed](#)]
35. Daniel, N.H.; Aravind, A.; Thakur, P. Are Ion Channels Potential Therapeutic Targets for Parkinson's Disease? *Neurotoxicology* **2021**, *87*, 243–257. [[CrossRef](#)] [[PubMed](#)]
36. Choudhury, S.P.; Bano, S.; Sen, S.; Suchal, K.; Kumar, S.; Nikolajeff, F.; Dey, S.K.; Sharma, V. Altered Neural Cell Junctions and Ion-Channels Leading to Disrupted Neuron Communication in Parkinson's Disease. *NPJ Park. Dis.* **2022**, *8*, 66. [[CrossRef](#)]
37. Miliukhina, I.V.; Usenko, T.S.; Senkevich, K.A.; Nikolaev, M.A.; Timofeeva, A.A.; Agapova, E.A.; Semenov, A.V.; Lubimova, N.E.; Totolyan, A.A.; Pchelina, S.N. Plasma Cytokines Profile in Patients with Parkinson's Disease Associated with Mutations in GBA Gene. *Bull. Exp. Biol. Med.* **2020**, *168*, 423–426. [[CrossRef](#)]

38. Pandey, M.K.; Burrow, T.A.; Rani, R.; Martin, L.J.; Witte, D.; Setchell, K.D.; McKay, M.A.; Magnusen, A.F.; Zhang, W.; Liou, B.; et al. Complement Drives Glucosylceramide Accumulation and Tissue Inflammation in Gaucher Disease. *Nature* **2017**, *543*, 108–112. [[CrossRef](#)]
39. Nagata, M.; Izumi, Y.; Ishikawa, E.; Kiyotake, R.; Doi, R.; Iwai, S.; Omahdi, Z.; Yamaji, T.; Miyamoto, T.; Bamba, T.; et al. Intracellular Metabolite  $\beta$ -Glucosylceramide Is an Endogenous Mincle Ligand Possessing Immunostimulatory Activity. *Proc. Natl. Acad. Sci. USA* **2017**, *114*, E3285–E3294. [[CrossRef](#)]
40. Schröder, M.; Kaufman, R.J. ER Stress and the Unfolded Protein Response. *Mutat. Res. Fundam. Mol. Mech. Mutagen.* **2005**, *569*, 29–63. [[CrossRef](#)]
41. Omura, T.; Kaneko, M.; Okuma, Y.; Matsubara, K.; Nomura, Y. Endoplasmic Reticulum Stress and Parkinson's Disease: The Role of HRD1 in Averting Apoptosis in Neurodegenerative Disease. *Oxid. Med. Cell. Longev.* **2013**, *2013*, 239854. [[CrossRef](#)]
42. da Costa, C.A.; El Manaa, W.; Duplan, E.; Checler, F. The Endoplasmic Reticulum Stress/Unfolded Protein Response and Their Contributions to Parkinson's Disease Physiopathology. *Cells* **2020**, *9*, 2495. [[CrossRef](#)]
43. Smith, L.; Schapira, A.H. GBA Variants and Parkinson Disease: Mechanisms and Treatments. *Cells* **2022**, *11*, 1261. [[CrossRef](#)]
44. Maor, G.; Rencus-Lazar, S.; Filocamo, M.; Steller, H.; Segal, D.; Horowitz, M. Unfolded Protein Response in Gaucher Disease: From Human to Drosophila. *Orphanet J. Rare Dis.* **2013**, *8*, 140. [[CrossRef](#)] [[PubMed](#)]
45. Kurzawa-Akanbi, M.; Hanson, P.; Blain, P.; Lett, D.; Mckeith, I.; Chinnery, P.; Morris, C. Glucocerebrosidase Mutations Alter the Endoplasmic Reticulum and Lysosomes in Lewy Body Disease. *J. Neurochem.* **2012**, *123*, 298–309. [[CrossRef](#)] [[PubMed](#)]
46. Schöndorf, D.C.; Aureli, M.; McAllister, F.E.; Hindley, C.J.; Mayer, F.; Schmid, B.; Sardi, S.P.; Valsecchi, M.; Hoffmann, S.; Schwarz, L.K.; et al. iPSC-Derived Neurons from GBA1-Associated Parkinson's Disease Patients Show Autophagic Defects and Impaired Calcium Homeostasis. *Nat. Commun.* **2014**, *5*, 4028. [[CrossRef](#)]
47. Sanchez-Martinez, A.; Beavan, M.; Gegg, M.E.; Chau, K.-Y.; Whitworth, A.J.; Schapira, A.H.V. Parkinson Disease-Linked GBA Mutation Effects Reversed by Molecular Chaperones in Human Cell and Fly Models. *Sci. Rep.* **2016**, *6*, 31380. [[CrossRef](#)] [[PubMed](#)]
48. Fernandes, H.J.R.; Hartfield, E.M.; Christian, H.C.; Emmanouilidou, E.; Zheng, Y.; Booth, H.; Bogetofte, H.; Lang, C.; Ryan, B.J.; Sardi, S.P.; et al. ER Stress and Autophagic Perturbations Lead to Elevated Extracellular  $\alpha$ -Synuclein in GBA-N370S Parkinson's iPSC-Derived Dopamine Neurons. *Stem Cell Rep.* **2016**, *6*, 342–356. [[CrossRef](#)] [[PubMed](#)]
49. Kuo, S.-H.; Tasset, I.; Cheng, M.M.; Diaz, A.; Pan, M.-K.; Lieberman, O.J.; Hutten, S.J.; Alcalay, R.N.; Kim, S.; Ximénez-Embún, P.; et al. Mutant Glucocerebrosidase Impairs  $\alpha$ -Synuclein Degradation by Blockade of Chaperone-Mediated Autophagy. *Sci. Adv.* **2022**, *8*, eabm6393. [[CrossRef](#)] [[PubMed](#)]
50. Usenko, T.S.; Bezrukova, A.I.; Bogdanova, D.A.; Nikolaev, M.A.; Miliukhina, I.V.; Gracheva, E.V.; Senkevich, K.A.; Zakharova, E.Y.; Emelyanov, A.K.; Pchelina, S.N. Gene Expression of Lysosomal Membrane Proteins in Parkinson Disease, Associated with Mutations in the Glucocerebrosidase Gene (Gba). *Ann. Clin. Exp. Neurol.* **2020**, *14*, 43–49. [[CrossRef](#)]
51. Heras-Sandoval, D.; Pérez-Rojas, J.M.; Hernández-Damián, J.; Pedraza-Chaverri, J. The Role of PI3K/AKT/MTOR Pathway in the Modulation of Autophagy and the Clearance of Protein Aggregates in Neurodegeneration. *Cell Signal.* **2014**, *26*, 2694–2701. [[CrossRef](#)]
52. Xu, F.; Na, L.; Li, Y.; Chen, L. RETRACTED ARTICLE: Roles of the PI3K/AKT/MTOR Signalling Pathways in Neurodegenerative Diseases and Tumours. *Cell Biosci.* **2020**, *10*, 54. [[CrossRef](#)] [[PubMed](#)]
53. Yeo, S.; Lim, S. Acupuncture Inhibits the Increase in Alpha-Synuclein by Modulating SGK1 in an MPTP Induced Parkinsonism Mouse Model. *Am. J. Chin. Med.* **2019**, *47*, 527–539. [[CrossRef](#)] [[PubMed](#)]
54. Gao, X.; Gao, Y.; Yan, H.; Liu, G.; Zhou, Y.; Tao, T.; Yue, T.; Pang, C.; Chen, X.; Gao, S.; et al. PDK4 Decrease Neuronal Apoptosis via Inhibiting ROS-ASK1/P38 Pathway in Early Brain Injury after Subarachnoid Hemorrhage. *Antioxid. Redox Signal.* **2021**, *36*, 505–524. [[CrossRef](#)]
55. Gao, X.; Gao, Y.-Y.; Wu, L.-Y.; Peng, Z.; Liu, X.-Z.; Chen, X.-X.; Gao, S.; Zhang, H.-S.; Lu, Y.; Hang, C.-H.; et al. High Expression of PDK4 Could Play a Potentially Protective Role by Attenuating Oxidative Stress after Subarachnoid Hemorrhage. *J. Clin. Med.* **2022**, *11*, 3974. [[CrossRef](#)]
56. Gong, J.; Zhang, L.; Zhang, Q.; Li, X.; Xia, X.-J.; Liu, Y.-Y.; Yang, Q.-S. Lentiviral Vector-Mediated SHC3 Silencing Exacerbates Oxidative Stress Injury in Nigral Dopamine Neurons by Regulating the PI3K-AKT-FoxO Signaling Pathway in Rats with Parkinson's Disease. *Cell Physiol. Biochem.* **2018**, *49*, 971–984. [[CrossRef](#)]
57. Castel, P.; Ellis, H.; Bago, R.; Toska, E.; Razavi, P.; Carmona, F.J.; Kannan, S.; Verma, C.S.; Dickler, M.; Chandarlapaty, S.; et al. PDK1-SGK1 Signaling Sustains AKT-Independent MTORC1 Activation and Confers Resistance to PI3K $\alpha$  Inhibition. *Cancer Cell* **2016**, *30*, 229–242. [[CrossRef](#)]
58. Liu, Z.; Chen, X.; Wang, Y.; Peng, H.; Wang, Y.; Jing, Y.; Zhang, H. PDK4 Promotes Tumorigenesis Through Activation of CREB-RHEB-MTORC1 Signaling Cascade. *J. Biol. Chem.* **2014**, *289*, 29739–29749. [[CrossRef](#)] [[PubMed](#)]
59. Pérez-Sisqués, L.; Sancho-Balsells, A.; Solana-Balaguer, J.; Campoy-Campos, G.; Vives-Isern, M.; Soler-Palazón, F.; Anglada-Huguet, M.; López-Toledano, M.-Á.; Mandelkow, E.-M.; Alberch, J.; et al. RTP801/REDD1 Contributes to Neuroinflammation Severity and Memory Impairments in Alzheimer's Disease. *Cell Death Dis.* **2021**, *12*, 616. [[CrossRef](#)] [[PubMed](#)]
60. Lv, X.; Hu, Y.; Wang, L.; Zhang, D.; Wang, H.; Dai, Y.; Cui, X.; Zheng, G. DDIT4 Mediates the Proliferation-Promotive Effect of IL-34 in Human Monocytic Leukemia Cells. *Blood Sci.* **2021**, *3*, 48–56. [[CrossRef](#)]

61. Malagelada, C.; Ryu, E.; Biswas, S.; Jackson-Lewis, V.; Greene, L. RTP801 Is Elevated in Parkinson Brain Substantia Nigral Neurons and Mediates Death in Cellular Models of Parkinson's Disease by a Mechanism Involving Mammalian Target of Rapamycin Inactivation. *J. Neurosci.* **2006**, *26*, 9996–10005. [[CrossRef](#)]
62. Verma, A.; Kommaddi, R.P.; Gnanabharathi, B.; Hirsch, E.C.; Ravindranath, V. Genes Critical for Development and Differentiation of Dopaminergic Neurons Are Downregulated in Parkinson's Disease. *J. Neural. Transm.* **2023**, *130*, 495–512. [[CrossRef](#)] [[PubMed](#)]
63. Li, C.C.; Wu, T.S.; Huang, C.F.; Jang, L.T.; Liu, Y.T.; You, S.T.; Liou, G.G.; Lee, F.J.S. GTP-Binding-Defective ARL4D Alters Mitochondrial Morphology and Membrane Potential. *PLoS ONE* **2012**, *7*, e43552. [[CrossRef](#)] [[PubMed](#)]
64. Chen, Q.; Weng, H.-Y.; Tang, X.-P.; Lin, Y.; Yuan, Y.; Li, Q.; Tang, Z.; Wu, H.-B.; Yang, S.; Li, Y.; et al. ARL4C Stabilized by AKT/MTOR Pathway Promotes the Invasion of PTEN-Deficient Primary Human Glioblastoma. *J. Pathol.* **2019**, *247*, 266–278. [[CrossRef](#)] [[PubMed](#)]
65. Dong, R.; Li, X.; Lai, K.O. Activity and Function of the Prmt8 Protein Arginine Methyltransferase in Neurons. *Life* **2021**, *11*, 1132. [[CrossRef](#)]
66. Bogetofte, H.; Ryan, B.J.; Jensen, P.; Schmidt, S.I.; Vergoossen, D.L.E.; Barnkob, M.B.; Kiani, L.N.; Chughtai, U.; Heon-Roberts, R.; Caiazza, M.C.; et al. Post-Translational Proteomics Platform Identifies Neurite Outgrowth Impairments in Parkinson's Disease GBA-N370S Dopamine Neurons. *Cell Rep.* **2023**, *42*, 112180. [[CrossRef](#)] [[PubMed](#)]
67. Grigor'eva, E.V.; Kopytova, A.E.; Yarkova, E.S.; Pavlova, S.V.; Sorogina, D.A.; Malakhova, A.A.; Malankhanova, T.B.; Baydakova, G.V.; Zakharova, E.Y.; Medvedev, S.P.; et al. Biochemical Characteristics of iPSC-Derived Dopaminergic Neurons from N370S GBA Variant Carriers with and without Parkinson's Disease. *Int. J. Mol. Sci.* **2023**, *24*, 4437. [[CrossRef](#)]
68. Mubariz, F.; Saadin, A.; Lingenfelter, N.; Sarkar, C.; Banerjee, A.; Lipinski, M.M.; Awad, O. Deregulation of MTORC1-TFEB Axis in Human iPSC Model of GBA1-Associated Parkinson's Disease. *Front. Neurosci.* **2023**, *17*, 1152503. [[CrossRef](#)]
69. Balestrino, R.; Tunesi, S.; Tesi, S.; Lopiano, L.; Zecchinelli, A.L.; Goldwurm, S. Penetrance of Glucocerebrosidase (GBA) Mutations in Parkinson's Disease: A Kin Cohort Study. *Mov. Disord.* **2020**, *35*, 2111–2114. [[CrossRef](#)]
70. Gan-Or, Z.; Dion, P.; Rouleau, G. Genetic Perspective on the Role of the Autophagy-Lysosome Pathway in Parkinson Disease. *Autophagy* **2015**, *11*, 1443–1457. [[CrossRef](#)]
71. Kinghorn, K.; Asghari, A.; Castillo-Quan, J. The Emerging Role of Autophagic-Lysosomal Dysfunction in Gaucher Disease and Parkinson's Disease. *Neural Regen. Res.* **2017**, *12*, 380–384. [[CrossRef](#)]
72. Zhang, Z.-N.; Hui, Z.; Chen, C.; Liang, Y.; Tang, L.-L.; Wang, S.-L.; Xu, C.-C.; Yang, H.; Zhao, Y.; Zhang, J.-S. Mechanism of Autophagy Regulation in MPTP-Induced PD Mice via the MTOR Signaling Pathway by Echinacoside. *Neuropsychiatr. Dis. Treat.* **2021**, *17*, 1397–1411. [[CrossRef](#)]
73. Wang, X.-W.; Yuan, L.-J.; Yang, Y.; Zhang, M.; Chen, W.-F. IGF-1 Inhibits MPTP/MPP + -Induced Autophagy on Dopaminergic Neurons through the IGF-1R/PI3K-Akt-MTOR Pathway and GPER. *Am. J. Physiol.-Endocrinol. Metab.* **2020**, *319*, E734–E743. [[CrossRef](#)]
74. Deng, H.; Ma, Z. Protective Effects of Berberine against MPTP-Induced Dopaminergic Neuron Injury through Promoting Autophagy in Mice. *Food Funct.* **2021**, *12*, 8366–8375. [[CrossRef](#)]
75. Rudenok, M.M.; Alieva, A.K.; Nikolaev, M.A.; Kolacheva, A.A.; Ugryumov, M.V.; Pchelina, S.N.; Slominsky, P.A.; Shadrina, M.I. Possible Involvement of Genes Related to Lysosomal Storage Disorders in the Pathogenesis of Parkinson's Disease. *Mol. Biol.* **2019**, *53*, 24–31. [[CrossRef](#)]
76. Lenihan, J.A.; Saha, O.; Heimer-McGinn, V.; Cryan, J.F.; Feng, G.; Young, P.W. Decreased Anxiety-Related Behaviour but Apparently Unperturbed NUMB Function in Ligand of NUMB Protein-X (LNx) 1/2 Double Knockout Mice. *Mol. Neurobiol.* **2017**, *54*, 8090–8109. [[CrossRef](#)] [[PubMed](#)]
77. Kovalev, G.I.; Vasileva, E.V.; Salimov, R.M. Comparison of Mouse Behavior in the Open Field, Closed and Elevated Cross-Maze Tests by the Use of Factor Analysis. *Zhurnal Vyss. Nervn. Deyatel'nosti Im. I.P. Pavlov.* **2019**, *69*, 123–130. [[CrossRef](#)]
78. Wang, L.; Wang, S.; Li, W. RSeQC: Quality Control of RNA-Seq Experiments. *Bioinformatics* **2012**, *28*, 2184–2185. [[CrossRef](#)] [[PubMed](#)]
79. Martin, M. Cutadapt Removes Adapter Sequences from High-Throughput Sequencing Reads. *EMBnet J.* **2011**, *17*, 10–12. [[CrossRef](#)]
80. Kim, D.; Langmead, B.; Salzberg, S.L. HISAT: A Fast Spliced Aligner with Low Memory Requirements. *Nat. Methods* **2015**, *12*, 357–360. [[CrossRef](#)]
81. Andrews, S. FastQC: A Quality Control Tool for High Throughput Sequence Data. Available online: <http://www.bioinformatics.babraham.ac.uk/projects/fastqc> (accessed on 5 June 2023).
82. Anders, S.; Pyl, P.T.; Huber, W. HTSeq—A Python Framework to Work with High-Throughput Sequencing Data. *Bioinformatics* **2015**, *31*, 166–169. [[CrossRef](#)]
83. Love, M.I.; Huber, W.; Anders, S. Moderated Estimation of Fold Change and Dispersion for RNA-Seq Data with DESeq2. *Genome Biol.* **2014**, *15*, 550. [[CrossRef](#)]
84. Bindea, G.; Mlecnik, B.; Hackl, H.; Charoentong, P.; Tosolini, M.; Kirilovsky, A.; Fridman, W.-H.; Pagès, F.; Trajanoski, Z.; Galon, J. ClueGO: A Cytoscape Plug-in to Decipher Functionally Grouped Gene Ontology and Pathway Annotation Networks. *Bioinformatics* **2009**, *25*, 1091–1093. [[CrossRef](#)] [[PubMed](#)]
85. Bindea, G.; Galon, J.; Mlecnik, B. CluePedia Cytoscape Plugin: Pathway Insights Using Integrated Experimental and in Silico Data. *Bioinformatics* **2013**, *29*, 661–663. [[CrossRef](#)]



86. Chi, J.-H.; Panner, A.; Cachola, K.; Crane, C.-A.; Murray, J.; Pieper, R.-O.; James, C.-D.; Parsa, A.-T. Increased expression of the glioma-associated antigen ARF4L after loss of the tumor suppressor PTEN. Laboratory investigation. *J. Neurosurg.* **2008**, *108*, 299–303. [[CrossRef](#)] [[PubMed](#)]
87. Lu, M.; Wang, J.; Jones, K.-T.; Ives, H.-E.; Feldman, M.-E.; Yao, L.J.; Shokat, K.-M.; Ashrafi, K.; Pearce, D. mTOR complex-2 activates ENaC by phosphorylating SGK1. *J. Am. Soc. Nephrol.* **2010**, *21*, 811–818. [[CrossRef](#)]
88. Zhang, Y.; Liu, L.; Hou, X.; Zhang, Z.; Zhou, X.; Gao, W. Role of Autophagy Mediated by AMPK/DDiT4/mTOR Axis in HT22 Cells Under Oxygen and Glucose Deprivation/Reoxygenation. *ACS Omega* **2023**, *8*, 9221–9229. [[CrossRef](#)] [[PubMed](#)]
89. Singh, M.; Shin, Y.-K.; Yang, X.; Zehr, B.; Chakrabarti, P.; Kandror, K.-V. 4E-BPs Control Fat Storage by Regulating the Expression of Egr1 and ATGL. *J. Biol. Chem.* **2015**, *290*, 17331–17338. [[CrossRef](#)]
90. Fruman, D.-A. mTOR signaling: New networks for ALL. *Blood* **2016**, *127*, 2658–2659. [[CrossRef](#)]
91. Wang, J.; Zhou, J.-Y.; Kho, D.; Reiners, J.-J., Jr.; Wu, G.S. Role for DUSP1 (dual-specificity protein phosphatase 1) in the regulation of autophagy. *Autophagy* **2016**, *12*, 1791–1803. [[CrossRef](#)]
92. Pinno, J.; Bongartz, H.; Klepsch, O.; Wundrack, N.; Poli, V.; Schaper, F.; Dittrich, A. Interleukin-6 influences stress-signalling by reducing the expression of the mTOR-inhibitor REDD1 in a STAT3-dependent manner. *Cell Signal* **2016**, *28*, 907–916. [[CrossRef](#)]
93. Mahajan, S.; Saini, A.; Chandra, V.; Nanduri, R.; Kalra, R.; Bhagyaraj, E.; Khatri, N.; Gupta, P. Nuclear Receptor Nr4a2 Promotes Alternative Polarization of Macrophages and Confers Protection in Sepsis. *J. Biol. Chem.* **2015**, *290*, 18304–18314. [[CrossRef](#)]

**Disclaimer/Publisher’s Note:** The statements, opinions and data contained in all publications are solely those of the individual author(s) and contributor(s) and not of MDPI and/or the editor(s). MDPI and/or the editor(s) disclaim responsibility for any injury to people or property resulting from any ideas, methods, instructions or products referred to in the content.